Effective Experimental Measurement and Constraint Quantification of J-R Curves for X80 Pipeline Steel ∀

X.K.Zhu[1], B.N. Leis[1], G. Shen[2] and W.R. Tyson[2]
[1] *Battelle Memorial Institute, Columbus, Ohio, USA*
[2] *CANMET Materials Technology Laboratory, Ottawa, Ontario, Canada*

Abstract: Effective and accurate experimental measurement of fracture toughness is critical to structural integrity assessment. Fracture testing to characterize toughness often adopts ASTM standard E1820 and the single edge-notched bend (SENB) specimen. For this specimen, the simultaneous measurement of load, load-line displacement (LLD), and crack mouth opening displacement (CMOD) are required in E1820, with CMOD used to obtain the compliance-based crack extension and LLD to evaluate the incremental value of *J*-integral. In this paper, a direct approach is introduced to determine more accurate *J* resistance curves for SENB specimens using only load-CMOD records. For constraint-dependent *J-R* curves obtained from fracture testing, J-A_2 fracture constraint theory is used to quantify the constraint effect on fracture toughness, so that laboratory test data can be transferred to practical engineering components.

Based on fracture toughness test data for X80 pipeline steel obtained using SENB specimens with different crack lengths from short to deep, constraint-dependent *J-R* curves are determined using the direct CMOD method and the E1820 LLD method. Comparison shows that these two methods agree well for all specimens considered. From these measured *J-R* curves, the constraint parameter A_2 is obtained for each specimen using finite element analysis and a constraint-corrected *J-R* curve is thus developed. It is concluded that the direct CMOD method is simple, effective and accurate for fracture toughness testing, and that the proposed constraint-corrected *J-R* curve can be used to transfer lab-measured fracture toughness to practical applications.

1. Introduction

Elastic-plastic fracture mechanics is one of the most important tools in structural integrity assessment for pipelines and pressure vessels. The *J*-integral based Resistance (*J-R*) curve, a measure of material fracture behavior, has been extensively used to characterize fracture resistance at crack initiation, crack growth, and tearing instability. Effective and accurate experimental measurement of *J*-integral based fracture toughness thus becomes essential for structural integrity or fitness-for-service assessment. Significant efforts have been devoted in the development of fracture testing methods for measuring the *J*-integral fracture toughness. A historic review on this topic can be found in Zhu et al. [1].

∀ Prepared for the 12th International Conference on Fracture, Ottawa, Canada, July 12-17, 2009

The current fracture toughness testing standard ASTM E1820 [2] uses the load-line displacement (LLD) based *J*-integral incremental equations developed by Ernst et al. [3] for evaluating the crack growth corrected *J*-integral. This LLD-based incremental equation requires the load, LLD, and crack length to determine *J*-integral for a growing crack. In E1820, the elastic unloading compliance method is adopted for the fracture testing to estimate crack length from the specimen compliance and crack-mouth-opening displacement (CMOD).

For the compact tension (CT) specimen geometry used in the fracture testing, CMOD gages sit on the load line. Thus, LLD can be determined directly via the CMOD clip gage. However, for single edge-notched bend (SENB) specimen geometry, CMOD and LLD must be independently measured. CMOD is used to determine compliance-based crack length, while LLD is used to determine incremental *J*-integral values. Consequently, this adds experimental complexity and expense in contrast to the CT specimen. To simplify experimental procedures and reduce the test costs, a direct approach was recently proposed by Zhu at al. [1], which allows determining the crack growth corrected *J*-integral directly from the load-CMOD data only, and the LLD is not needed.

Because *J-R* curves depend on constraint levels at the crack tip due to different loading and geometry configurations, constraint dependence is a practical issue in transferring experimental results measured using standard laboratory specimens to defect assessment in actual components. Standard specimens as specified in ASTM E1820 have strict size requirements to ensure high constraint levels at the crack tip, while the non-standard specimens or surface-cracked components usually involve low constraint levels. In cases where *J-R* curves are developed using high-constraint specimens, its use in design or defect-severity analysis will tend to be conservative. Conversely, cases where toughness data is obtained from specimens whose constraint is less than the application would result in a non-conservative outcome. As a result, it is important to quantify constraint effects on the *J-R* curves, so laboratory data can be transferred to practical applications with appropriate constraint.

It has been recognized from numerical analyses that fracture constraint is due to the loss of the single-parameter *J*-integral dominance, which has let to the development of several two-parameter fracture theories. Two examples include the *J-Q* theory proposed by O'Dowd and Shih [4] and the J-A_2 three-term solution proposed by Yang et al. [5], where Q and A_2 are constraint parameters. These two fracture constraint theories have been demonstrated useful for fracture assessment of pipelines by Zhu and Leis [6, 7] and Shen et al. [8].

Based on experimental data from toughness testing, this paper develops *J-R* curves for X80 pipeline steel and compares the outcome in terms of the E1820 LLD incremental method and the direct CMOD method [1]. Consistent with E1820, crack extension was measured using the elastic unloading compliance method for a set of SENB specimens hose crack length was varied from short to deep to study crack-tip constraint effects on the *J-R* curves. The *J-A_2* fracture constraint theory is adopted with the parameter A_2 being used to quantify the constraint effect on the experimental results. A constraint-corrected *J-R* curve for this pipeline steel is thus developed.

2. Experimental Determination of J-Resistance Curves

2.1. LLD-based incremental method

In ASTM E1820 [2], standard method for developing a *J-R* curve from a single specimen test uses elastic unloading compliance technique to measure crack extension and LLD incremental equation to evaluate *J*-integral. When using SENB specimens, the incremental evaluation requires simultaneous measurement of load (P), load-line displacement (LLD or Δ), and crack mouth opening displacement (CMOD or V) in a single test. As indicated above, the P-CMOD data determine compliance-based crack length or crack extension, and P-LLD data combined with the crack length determine the *J*-integral values. At a loading point *i*, since the load P_i, the load-line displacement Δ_i, and the crack length a_i are known, the total *J*-integral is calculated from elastic and plastic components:

$$J_i = J_{el(i)} + J_{pl(i)} \tag{1}$$

where the elastic component J_{el} and the plastic component J_{pl} are determined by:

$$J_{el(i)} = \frac{\left[K_i(a_i)\right]^2(1-\nu^2)}{E} \tag{2}$$

$$J_{pl(i)} = \left(J_{pl(i-1)} + \frac{\eta_{LLD}^{i-1}}{b_{i-1}B_N} A_{\Delta_{pl}}^{i-1,i}\right)\left(1 - \frac{\gamma_{LLD}^{i-1}}{b_{i-1}}(a_i - a_{i-1})\right) \tag{3}$$

where $A_{\Delta_{pl}}^{i-1,i}$ denotes the incremental area under the $P - \Delta_{pl}$ curve from loading point *i*-1 to *i*, and is expressed as:

$$A_{\Delta_{pl}}^{i-1,i} = \frac{1}{2}\left(P_i + P_{i-1}\right)\left(\Delta_{pl}^{i} - \Delta_{pl}^{i-1}\right) \tag{4}$$

Equation (3) is the LLD-based incremental *J*-integral equation proposed by Ernst et al. [3] based on the deformation theory of plasticity. Since it considers a crack growth correction, this incremental *J*-integral equation is considered "accurate" in calculation of the *J*-integral for a growing crack.

For the standard SENB specimens with deep cracks of $0.45 \le a/W \le 0.7$, E1820-06 [2] used $\eta_{LLD} = 1.9$ and $\gamma_{LLD} = 1.0$ (should be 0.9). For non-standard SENB specimens with shorter cracks, these two geometry factors vary with *a/W*. Recently, Zhu et al. [1] proposed a general expression:

$$\eta_{LLD} = 1.620 + 0.850(a/W) - 0.651(a/W)^2, \qquad 0.25 \le a/W \le 0.7 \tag{5}$$

It is found that the η_{LLD} in Eq. (5) is very close to 1.9, as used in E1820-06.

2.2. CMOD-based incremental method

A direct procedure to evaluate the *J*-integral from incremental load versus CMOD data was developed by Zhu et al. [1], which is briefly presented now for use later in this paper. Based on the deformation theory of plasticity and the energy principle, a CMOD-based incremental *J*-integral equation at loading point *i* was proposed in the form:

$$J_{pl(i)} = \left(J_{pl(i-1)} + \frac{\eta_{CMOD}^{i-1}}{b_{i-1}B_N} A_{V_{pl}}^{i-1,i} \right)\left(1 - \frac{\gamma_{CMOD}^{i-1}}{b_{i-1}}(a_i - a_{i-1}) \right) \tag{6}$$

In this equation $A_{V_{pl}}^{i-1,i}$ denotes the incremental area under the measured P-V_{pl} curve, which is calculated by:

$$A_{V_{pl}}^{i-1,i} = \frac{1}{2}(P_i + P_{i-1})(V_{pl}^i - V_{pl}^{i-1}) \tag{7}$$

The elastic component and total value of the *J*-integral continue to be determined by Eqs (1) and (2). Similar to Eq. (3), the γ_{CMOD} term serves as the crack growth correction. Eq. (6) can be used for any specimen, provided that the geometry factors η_{CMOD} and γ_{CMOD} are known. Because LLD and CMOD are equal for the CT specimen, the incremental equations, i.e., Eqs. (3) and (6), become identical.

A modified expression for η_{CMOD} was recently obtained by Zhu et al. [1] as:

$$\eta_{CMOD} = 3.667 - 2.199(a/W) + 0.437(a/W)^2, \qquad 0.1 \le a/W \le 0.7 \tag{8}$$

This equation is accurate over the full range of *a/W* considered by E1820. The expression for γ_{CMOD} corresponding to the proposed η_{CMOD} in Eq. (8) is:

$$\gamma_{CMOD} = 0.131 + 2.131(a/W) - 1.465(a/W)^2, \qquad 0.25 \le a/W \le 0.7 \tag{9}$$

2.3. Experimental results and analyses

A set of SENB specimens were tested by Shen et al. [9] for the X80 pipeline steels consistent with E1820. Grade X80 (N550) is a higher strength pipeline steel, supplied from typical line pipe by TransCanada Pipelines Ltd. (TCPL). According to tensile tests for this X80 steel, the 0.2% offset yield stress is 570 MPa, the 0.5% total yield stress is 576 MPa, the ultimate tensile stress is 675 MPa, the elongation for the one inch (25mm) gage length is 42.2% and the final reduction of area is 68.3%.

After fatigue pre-cracking, the SENB specimens were side grooved to a total thickness reduction of 20%, in an attempt to develop plane strain conditions along the crack front. The specimen width *W* is 23 mm, the thickness *B* is 11.5 mm, the span is 92 mm, and the initial crack length *a* varies so that the *a/W* lies between 0.24 and 0.64. All specimens were cut from the line pipe in L-C orientation, and tested in three-point bending at room temperature (about 20^{o}C).

After testing, the specimens were heat tinted and then broken in liquid nitrogen. The initial and final crack lengths were measured on the fracture surface using the 9-point technique as described in E1820. The criterion for uniform crack extension given in E1820 was not met for the final crack length, primarily because splitting occurred. For some specimens with severe splitting, the difference among the nine physical measurements for the final crack length was as high as 40%. However, splitting was not observed for crack extension $\Delta a \leq 0.2$ mm.

The standard elastic unloading compliance method was used in all the fracture tests to determine the instantaneous crack length. For each specimen, the load, LLD and CMOD data were simultaneously recorded during the test. Figures 1(a) and 1(b) show the raw load-LLD records and load-CMOD records, respectively, for initial crack lengths a_0 / W = 0.24, 0.25, 0.42, 0.43, 0.63 and 0.64. These figures indicate that for each test the LLD is greater than the CMOD at a given loading point, and that the *P*-LLD curve is relatively more abrupt with the onset of tearing than the *P*-CMOD curve. Note that the CMOD data for a_0/W = 0.43

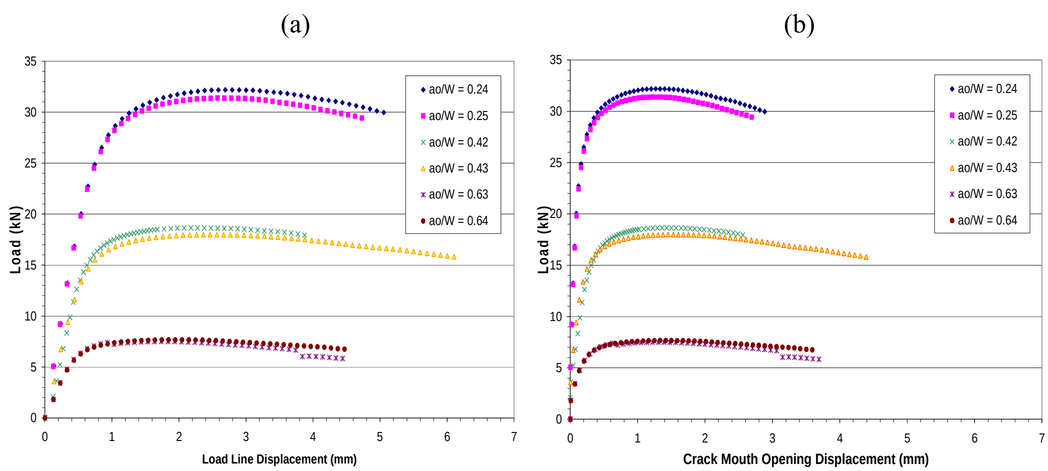

Figure 1. Experimental data for X80 SENB specimens (a) P-LLD; (b) P-CMOD

were estimated from the corresponding LLD data using the technique developed in Reference 10. Recently, Zhu et al. [11] estimated the crack extension and *J-R* curves using the LLD data and the normalization method. Good agreement apparent between their estimated and measured results implies that these test data are accurate.

The value of *J*-integral was calculated for each specimen using crack length and *P*-LLD record via Eqs (1), (2) and (3). It has likewise been calculated via Eqs (1), (2) and (6) using crack length and the *P*-CMOD record. Figures 2(a) and 2(b) compare the *J-R* curves determined using the LLD- and CMOD-based equations, respectively, for a deep crack (a_0 / W = 0.64) and a short crack (a_0 / W = 0.25). It is observed from these figures that the outcome of the direct CMOD method agrees well with the standard LLD method, although the direct method leads to results slightly greater than for the LLD method. Error analysis [1] indicates this is expected because the CMOD based *J*-integral increment is slightly larger than that for the LLD method.

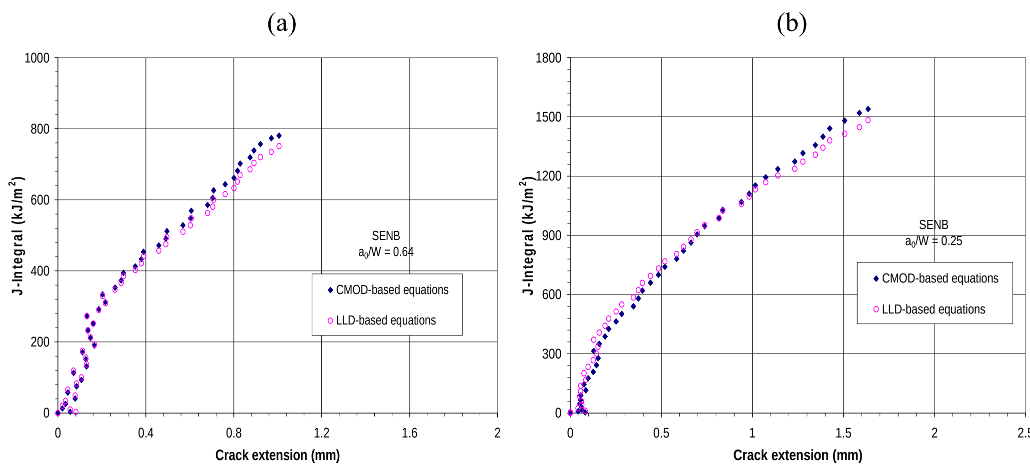

Figure 2. Comparisons of *J-R* curves from LLD and CMOD methods.
(a) a_0/W = 0.64, (b) a_0/W = 0.25

Figures 3(a) and 3(b) show the experimental *J-R* curves determined, respectively, using the E1820 LLD method and the direct CMOD method for all six results developed for the X80 SENB specimens. Note that the blunting line and the 0.2 mm offset line are also shown in these figures. Within the crack extension of 1 mm, the *J-R* curves determined by the two methods are nearly identical across this group of specimens. This infers that the fracture toughness at crack initiation determined using the direct CMOD method is equivalent to that using the standard LLD method. In addition, it is observed that the scatter range of *J-R* curves in Fig. 3(b) is almost similar to that in Fig. 3(a).

(a) (b)

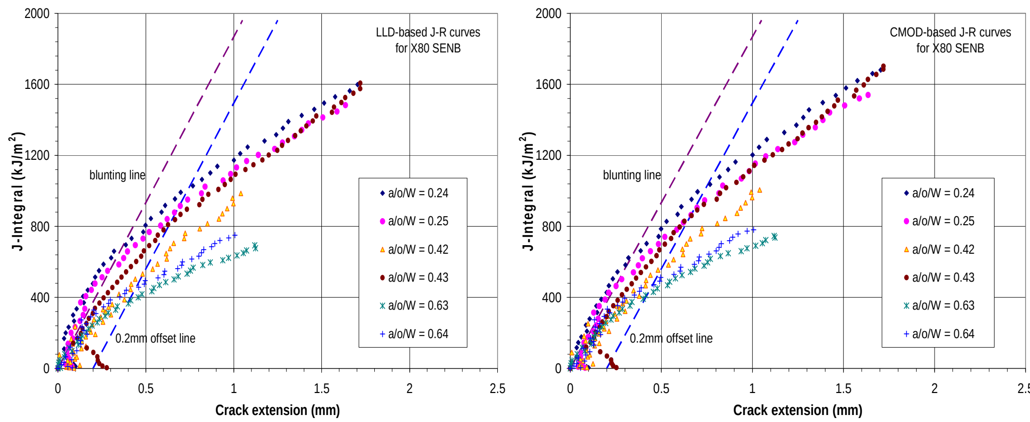

Figure 3. Final experimental *J-R* curves for X80 (a) LLD-based, (b) CMOD-based

3. Constraint Quantification for these *J*-R Curves

3.1. The J-A_2 solution

The *J*-A_2 three-term solution proposed by Yang et al. [5] was adopted earlier to characterize the crack-tip field and quantify the constraint level for all specimens considered. In this context, the asymptotic stress field near the crack tip under plane strain conditions has the form:

$$\frac{\sigma_{ij}}{\sigma_0} = A_1\left[\left(\frac{r}{L}\right)^{s_1}\tilde{\sigma}_{ij}^{(1)}(\theta) + A_2\left(\frac{r}{L}\right)^{s_2}\tilde{\sigma}_{ij}^{(2)}(\theta) + A_2{}^2\left(\frac{r}{L}\right)^{s_3}\tilde{\sigma}_{ij}^{(3)}(\theta)\right] \tag{10}$$

where the stress angular functions $\tilde{\sigma}_{ij}^{(k)}(\theta)$ (k=1, 2, 3) and the stress exponents s_k ($s_1 < s_2 < s_3$) depend on the strain hardening exponent n only. The characteristic length parameter L has been taken as 1 mm. The parameter A_1 is related to the J driving force, while $s_1 = -1/(n+1)$ and $s_3 = 2s_2 - s_1$ for $n \geq 3$. The constraint parameter A_2 is an unknown constant that is determined by matching the opening stress from the *J*-A_2 solution with FEA results at $r/(J/\sigma_0) = 1 \sim 2$, for example.

For deep crack bending specimens under large scale yielding (LSY), it has been shown that the global bending stress significantly affects the crack-tip field. As a result, the *J*-A_2 three-term solution in Eq. (10) fails to correctly describe the crack-tip field. To eliminate the influence of the global bending stress on the asymptotic crack-tip stress field, Chao et al. [12] recently developed a modification of the *J*-A_2 solution for the crack opening stress ahead of the crack tip, i.e. at $\theta = 0^{\circ}$, in bending specimens as follows:

$$\frac{\sigma_{\theta\theta}(0)}{\sigma_0} = A_1\left[\left(\frac{r}{L}\right)^{s_1}\tilde{\sigma}^{(1)}_{\theta\theta}(0) + A_2\left(\frac{r}{L}\right)^{s_2}\tilde{\sigma}^{(2)}_{\theta\theta}(0) + A_2{}^2\left(\frac{r}{L}\right)^{s_3}\tilde{\sigma}^{(3)}_{\theta\theta}(0)\right] - \frac{6Mr}{\sigma_0 b^3} \tag{11}$$

where M is the global bending moment. The modified J-A_2 solution still only involves two parameters, namely the applied loading (J and M) and the constraint parameter (A_2).

3.2. Determination of constraint parameters

Detailed plane strain elastic-plastic finite element analysis (FEA) has been performed by Zhu and Leis [7] for the X80 SENB specimens, in order to calculate the crack-tip stress and strain fields and determine constraint parameters for the test specimens. The parameter A_2 is extracted from the FEA opening stress at the crack tip when the specimen loading reaches the initiation toughness, where the deformation involves LSY and so A_2 attains a nearly constant value.

The FEA results performed in Ref. [7] showed that the A_2 values obtained using Eq. (10) are nearly the same and hold constant for all loading for the short cracks, but are different for the deeper cracks under LSY. After the global bending influence was considered, the value of A_2 obtained from Eq. (11) is a nearly load-independent constant for both short and deep cracked specimens. Specifically, $A_2 \approx -0.274$, -0.213 and -0.178, respectively for $a/W = 0.24$, 0.42, and 0.64. These results indicate that it is reasonable to use the load-independent parameter A_2 to quantify the constraint level of the *J-R* curve for SENB specimen.

3.3. Constraint-corrected J-R curves

As noted above the constraint parameter A_2 is effectively load-independent such that the value of A_2, determined for example at the crack initiation, can be throughout subsequent stable crack growth. For this reason, A_2 is an appropriate parameter for quantifying the effects of constraint on the *J-R* response. Under J-A_2 controlled crack growth, the J-integral resistance curve can be expressed by a power-law relationship as suggested in References 6 and 7. Thus:

$$J(\Delta a, A_2) = C_1(A_2)\left(\frac{\Delta a}{k}\right)^{C_2(A_2)} \tag{12}$$

where k = 1 mm, the coefficients $C_1(A_2)$ and $C_2(A_2)$ are as yet undetermined functions of A_2. Once the functional forms of $C_1(A_2)$ and $C_2(A_2)$ are obtained, a family of constraint-corrected *J-R* curves is completely determined.

Two equations to determine the coefficients $C_1(A_2)$ and $C_2(A_2)$ can be established at any two convenient values of crack extension based on experimental *J*-R curves. For present purposes the first point is taken at crack extension Δa_1, i.e., at initiation, and the second is taken after crack extension Δa_2 beyond initiation. The corresponding J-integrals are denoted by $J\big|_{\Delta a_1} = J_{\Delta a_1}(A_2)$, $J\big|_{\Delta a_2} = J_{\Delta a_2}(A_2)$, where $J_{\Delta a_1}(A_2)$ and $J_{\Delta a_1}(A_2)$ are two known functions of A_2, and determined by best-fitting test data extracted from at least three experimental J-R curves. Application of Eq. (12) leads to the following:

$$
\begin{aligned}
C_1(A_2)(\Delta a_1 / k)^{C_2(A_2)} &= J_{\Delta a_1}(A_2) \\
C_1(A_2)(\Delta a_2 / k)^{C_2(A_2)} &= J_{\Delta a_2}(A_2)
\end{aligned}
\tag{13}
$$

In principle, if Δa_i (i = 1-2) is chosen between 0.2 and 2 mm, it automatically satisfies the ASTM E 1820 criterion for acceptable data. Equations (13) can be used to determine C_1 and C_2 for a given A_2. The valid range of A_2, based on past studies, is between -1 and 0, as the crack tip constraint varies from low to high. Solving for C_1 and C_2 within this range of A_2 defines the functional dependence of C_1 and C_2 on A_2. Finally, least-squares regression analysis provides the desired functions of C_1 and C_2 with A_2.

Using the desired experimental J-R curves shown in Fig. 3(b) and following the procedures described above, a constraint corrected J-R curve in terms of A_2 can be constructed for X80 pipeline steel. Using the (modified) J-A_2 solution at $J_{0.2\text{mm}}$, the value of A_2 for each SENB specimen was determined using the finite element analysis in section 3.2. Two equations similar to Eq. (13) are then set up to solve for C_1 and C_2 at $J = J_{0.2\text{mm}}$ and $J = J_{1.0\text{mm}}$. Finally, the constraint-corrected J-R curve for X80 pipeline steel is obtained as:

$$
J(\Delta a,\ A_2) = -4417.1 A_2 \left(\frac{\Delta a}{1\,\text{mm}} \right)^{0.668}
\tag{14}
$$

where the J-integral has units of kJ/m^2. As evident in Eq. (14), the constraint corrected J-R curve is a function of A_2 and Δa. If A_2 is known for a specific geometry, the J-R curve can be easily predicted from Eq. (14).

For the tested SENB specimens with a/W = 0.24, 0.42 and 0.64, the value of A_2 was determined at the averaged $J_{0.2\text{mm}} \approx 337.3$ kJ/m^2 as -0.274, -0.213 and -0.178, respectively. The corresponding J-R curves are thus predicted using Eq. (14). Figure 4 compares the predicted J-R curves with the experimental J-R curves for the three SENB specimens. The results show that the predicted J-R curves match well with the experimental data. Therefore, the constraint-corrected J-R curve or Eq. (14) can be used to reproduce or predict the J-R curve for any specimen or actual component, provided that the constraint parameter A_2 for that geometry is known a priori.

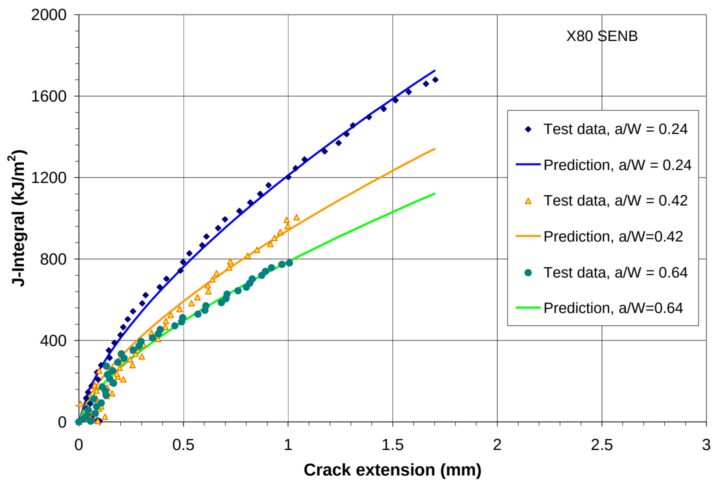

Figure 4. Comparison of experimental and predicted *J-R* curves for *a/W*=0.24, 0.42 and 0.64

4. Conclusions

The accurate experimental measurement and constraint quantification of *J*-integral based resistance curves were investigated using the SENB specimens for X80 pipeline steel. Both the ASTM E1820 LLD incremental method and the direct CMOD method were considered to determine crack growth corrected *J-R* curves, as the basis to evaluate their accuracy. Based the fracture test data from the X80 SENB specimens, constraint-dependent *J-R* curves were obtained using the two methods.

The results showed that the direct CMOD method agreed well with the standard LLD method for all SENB specimens considered. Because CMOD can be measured more easily and accurately than LLD, the direct method enables a simpler experimental procedure with associated cost savings and more accurate crack growth corrected *J-R* curves as compared to the LLD method. The constraint parameter A_2 was obtained for each specimen in reference to finite element analysis, the experimental *J-R* curves, and J-A_2 fracture constraint theory. A family of constraint-corrected *J-R* curves was then developed for the X80 pipeline steel. From detailed analyses and comparisons presented, it is concluded that the direct CMOD method is simple, effective and accurate for the fracture toughness testing. The proposed constraint-corrected *J-R* curve can reasonably characterize fracture resistance, and thus facilitates transferability of fracture toughness into practical applications involving comparable X80 pipeline steel.

Note that caution must be exercised in directly applying the results from bend testing to practical applications involving tensile loading, because of the influence of the bending term in the former case. The stress gradient in the fracture process zone at the crack tip is different in tension and in bending, and this affects fracture constraint and micromechanisms. Recently, Shen et al. [8] showed that both the gradients of the crack-tip stress field and the crack-tip constraint (A_2 or Q) for a single-edge notched tension (SENT) specimen are close to those for circumferential flaws in a pipe with the same depth as in SENT samples. As a result, test results for the SENT specimens could be directly applied to actual pipelines with circumferential cracks. Such direct application is simpler than the proposed constraint correction method.

References

[1] X.K. Zhu, B.N. Leis and J.A. Joyce, Experimental estimation of J-R curves from load-CMOD records for SE(B) specimens, *J ASTM Intl*, 5(5), 2008: Paper ID JAI101532.

[2] ASTM E1820-06, Standard test method for measurement of fracture toughness, *Annual Book of ASTM Standards*, Vol. 03.01, 2006.

[3] H.A. Ernst, P.C Paris. and J.D. Landes, Estimations on J-integral and tearing modulus *T* from a single specimen test record, ASTM STP 743, 1981, pp. 476-502.

[4] N.P. O'Dowd and C.F. Shih, Family of crack-tip fields characterized by a triaxiality parameter — I. Structure of Fields, *J Mech Phys Solid*, 39, 1991, 989-1015.

[5] S.Yang, Y.J. Chao and M.A. Sutton, Higher-order asymptotic fields in a power-law hardening material, *Engng Fract Mech*, 45, 1993, 1-20.

[6] X.K. Zhu and B.N. Leis, Constraint corrected J-R curve and its applications to fracture assessment for X80 pipelines, *J ASTM Intl*, 3(6), 2006: Paper ID JAI13209.

[7] X.K. Zhu and B.N. Leis, Application of constraint-corrected *J-R* curve to fracture analysis of pipelines, *J Pres Ves Tech*, 128, 2006, 581-589.

[8] G. Shen, R. Bouchard, J.A. Gianetto and W.R. Tyson, Fracture toughness evaluation of high strength steel pipe, *Proc ASME PVP Conference*, July 27-23, 2008, Chicago, USA: PVP2008-61100.

[9] G. Shen, W.R. Tyson, A. Glover, and D. Horsley, Constraint effects on linepipe toughness, *Proc the 4th Int Conf on Pipeline Technology*, Vol. 2, May 9-13, 2004, Ostend, Belgium, pp.703-720.

[10] X.K. Zhu and B.N. Leis, Experimental determination of J-R curves using SENB specimens and P-CMOD data, *Proc ASME PVP Conf*, July 27-23, 2008, Chicago, USA: PVP2008-61219.

[11] X.K. Zhu, B.N. Leis, G. Shen and W.R. Tyson, Experimental determination of constraint dependent J-R curves for X80 pipeline steel using the normalization method, *Proc ASME Intl Mech Engng Cong Exp*, Nov 5-10, 2006, Chicago, USA: IMECE2006-13180.

[12] Y.J. Chao, X.K. Zhu, Y. Kim, P.S. Lam, M.J. Pechersky, and M.J. Morgan, Characterization of Crack-Tip Fields and Constraints for Bending Specimens under Large-Scale Yielding, *Intl J Fract*, 127, 2004, 283-302.